Glycobiology, 2022, **32**, 5, 391–403
https://doi.org/10.1093/glycob/cwab133
Advance access publication date 24 December 2021
Original Article

Characterization of the ganglioside recognition profile of *Escherichia coli* heat-labile enterotoxin LT-IIc

Dani Zalem[1,6], Martin Juhás[1,5,6], Manuela Terrinoni[2], Natalie King-Lyons[3], Michael Lebens[2], Annabelle Varrot[4], Terry D Connell[3], Susann Teneberg[1,*]

[1]Department of Medical Biochemistry and Cell Biology, Sahlgrenska Academy, Institute of Biomedicine, University of Gothenburg, Sweden, [2]Department of Microbiology and Immunology, Sahlgrenska Academy, Institute of Biomedicine, University of Gothenburg, Sweden, [3]Department of Microbiology & Immunology and The Witebsky Center for Microbial Pathogenesis and Immunology, The Jacobs School of Medicine and Biomedical Sciences, The University at Buffalo, State University of New York, Buffalo, NY 14203, USA, [4]University Grenoble Alpes, CNRS, CERMAV, Grenoble 38000 France, [5]Present address: Department of Pharmaceutical Chemistry and Pharmaceutical Analysis, Charles University, Faculty of Pharmacy in Hradec Králové, Akademika Heyrovského 1203, Hradec Králové 500 05, Czech Republic

*Corresponding author: e-mail: Susann.Teneberg@medkem.gu.se
[6]These authors contributed equally to this work.

The heat-labile enterotoxins of *Escherichia coli* and cholera toxin of *Vibrio cholerae* are related in structure and function. Each of these oligomeric toxins is comprised of one A polypeptide and five B polypeptides. The B-subunits bind to gangliosides, which are followed by uptake into the intoxicated cell and activation of the host's adenylate cyclase by the A-subunits. There are two antigenically distinct groups of these toxins. Group I includes cholera toxin and type I heat-labile enterotoxin of *E. coli*; group II contains the type II heat-labile enterotoxins of *E. coli*. Three variants of type II toxins, designated LT-IIa, LT-IIb and LT-IIc have been described. Earlier studies revealed the crystalline structure of LT-IIb. Herein the carbohydrate binding specificity of LT-IIc B-subunits was investigated by glycosphingolipid binding studies on thin-layer chromatograms and in microtiter wells. Binding studies using a large variety of glycosphingolipids showed that LT-IIc binds with high affinity to gangliosides with a terminal Neu5Acα3Gal or Neu5Gcα3Gal, e.g. the gangliosides GM3, GD1a and Neu5Acα3-/Neu5Gcα3–neolactotetraosylceramide and Neu5Acα3-/Neu5Gcα3-neolactohexaosylceramide. The crystal structure of LT-IIc B-subunits alone and with bound LSTd/sialyl-lacto-*N*-neotetraose d pentasaccharide uncovered the molecular basis of the ganglioside recognition. These studies revealed common and unique functional structures of the type II family of heat-labile enterotoxins.

Key words: b-subunit crystal structure; B-subunit; carbohydrate binding; ganglioside recognition; heat-labile enterotoxin LT-IIc.

Introduction

Enterotoxigenic *Escherichia coli* (ETEC) is responsible for endemic diarrhea in low-income countries and for the majority of all moderate to severe travellers' diarrheal infections (Gascon 2006; Lamberti et al. 2014; Kotloff et al. 2017). The elicited diarrheal symptoms are mainly due to the action of enterotoxins released from the bacteria. Both heat-stable and heat-labile (LTs) enterotoxins are produced by ETEC. The heat-labile enterotoxins belong to AB_5 toxins family, a group of oligomeric proteins consisting of an A-subunit with catalytic activity and a pentameric B-subunit mediating binding to host glycoconjugates (Fan et al. 2000; Beddoe et al. 2010).

The heat-labile enterotoxins are divided into two major groups based on genetic, biochemical and immunological characteristics. The type I subfamily consists of LT-I enterotoxin of *E. coli*, which is closely related to cholera toxin (CT), and other related enterotoxins from bacteria such as *Campylobacter jejuni*, whereas the type II subfamily is comprised of three members, which are denoted LT-IIa, LT-IIb and LT-IIc (Hajishengallis and Connell 2013). The amino acid sequences of LT type II A-subunits have 50–60% identity with the A-subunits of CT/LT-I, whereas there is a very low amino acid homology (<14% identity) between the type II B-subunits and the B-subunits of CT and LT-I (van den Akker et al. 1996).

The differences in amino acid sequences of the B-subunits are reflected in their different carbohydrate binding preferences. The primary receptor of the B-subunits of CT and LT-I is the GM1 ganglioside (Holmgren 1973); LT-I also binds to glycoconjugates with terminal *N*-acetyllactosamine (Orlandi et al. 1994; Teneberg et al. 1994). The initial binding studies with type II B-subunits were focused on gangliosides with ganglio (Galβ3GalNAc) core chains and demonstrated that although LT-IIa B-subunits bind with highest affinity for the GD1b ganglioside, the B-subunits of LT-IIb interact with the gangliosides GD1a and GT1b (Fukuta et al. 1988), and the gangliosides recognized by LT-IIc B-subunits are GM1, GM2, GM3 and GD1a (Nawar et al. 2010; Berenson et al. 2013). More recent binding studies have demonstrated that the B-subunits of LT-IIb also bind to gangliosides with neolacto (Galβ4GlcNAc) core chains (Zalem et al. 2016).

Despite of the very limited sequence identity, the overall structure of the LT-IIb holotoxin closely resembles that of CT and LT-I (van den Akker et al. 1996). Recently the crystal

Received: October 22, 2021. **Revised:** November 23, 2021. **Accepted:** December 19, 2021

structure of the B-subunits of LT-IIb with bound Neu5Acα3-neolactotetraose demonstrated that the ganglioside binding site of LT-IIb is located in the same region as the GM1 binding sites of CT and LT type I (Zalem et al. 2016). The Neu5Ac moiety, however, is rotated ∼120° in LT-IIb compared with the moiety in CT and LT-I, and the orientation of the carbohydrate chain, and therefore the network of contacts, is entirely different. Furthermore, it was demonstrated that there are two Neu5Ac binding sites within the LT-IIb B-subunits. A secondary binding site in the vicinity of the primary site has not been found in the B-subunits of CT and LT-I.

The current study aimed to determine if two binding sites within one monomer were a unique feature of LT-IIb or if the pattern was also present in the other type II B-subunits. First, the carbohydrate binding specificity of LT-IIc was more precisely investigated using our collection of gangliosides of various core chain series from different sources. Ganglio series gangliosides were recognized by the B subunits of LT-IIc, with preferential binding to GD1a, as previously described (Nawar et al. 2010; Berenson et al. 2013). In addition, the LT-IIc B-subunits bound to neolacto core gangliosides, e.g. Neu5Acα3nLc$_4$Cer and Neu5Gcα3nLc$_6$Cer. To obtain more atomic details of the binding characteristics of LT-IIc, we determined the crystal structure of LT-IIc B-subunits in apo form and in complex with the LSTd/sialyl-lacto-*N*-neotetraose d pentasaccharide.

Results

Screening for LT-IIc carbohydrate recognition by binding to glycosphingolipid mixtures on thin-layer chromatograms

In the first series of experiments, the binding of LT-IIc B-subunits to a number of well-characterized glycosphingolipid fractions from different sources was evaluated. All glycosphingolipid binding studies were performed using ^{125}I-labeled B-subunits. No binding to nonacid glycosphingolipids was detected (not shown), but in the acid fractions, several binding-active compounds were revealed (exemplified in Figure 1B). In comparison, the binding pattern obtained with CT B-subunits (Figure 1D) was much more restricted.

The major glycosphingolipids in the acid fraction from human small intestine (lane 1) are sulfatide and the gangliosides Neu5Ac-GM3 and Neu5Ac-GD3. There are also minor compounds such as Neu5Acα3-neolactotetra- and Neu5Acα3-neolactohexaosylceramide (Zalem et al. 2016). There was no binding of LT-IIc in the sulfatide region, whereas the LT-IIc bound to several compounds migrating as the GM3 ganglioside and below (Figure 1B, lane 1). The acid fraction in lane 2 (human neutrophils) and lane 3 (rabbit thymus) contained the GM3 ganglioside and gangliosides with neolacto core chain (Iwamori and Nagai 1981; Stroud et al. 1996a; Stroud et al. 1996b), and with Neu5Ac in the case of human neutrophil gangliosides and Neu5Gc in the rabbit thymus gangliosides. Several bands were detected in both lanes indicating that gangliosides with neolacto core chain are recognized by LT-IIc B-subunits. The major ganglioside of bovine buttermilk (lane 5) is Neu5Ac-GD3 (Hauttecoeur et al. 1985). No binding was obtained at the level of binding of anti-GD3 antibodies (Figure 1C, lane 5), suggesting that the GD3 ganglioside is nonbinding. The acid fraction from goat erythrocytes (lane 6) is a complex mixture of Neu5Gc-terminated gangliosides, like Neu5Gc-GD3, Neu5Gc-neolactotetra- and Neu5Gc-neolactohexaosylceramide, and Neu5Gc-GD1b (S. Teneberg, unpublished data). Several slow migrating gangliosides in this fraction were recognized by the LT-IIc B-subunits.

Detailed dissection of LT-IIc ganglioside recognition profile

Binding assays with pure reference glycosphingolipids in defined amounts were subsequently performed to define the carbohydrate recognition specificity of the LT-IIc B-subunits. In the initial assays, relatively high amounts of glycosphingolipids (2–4 μg) were applied on the chromatograms. The LT-IIc B-subunits then bound to almost all glycosphingolipids in an unspecific manner. Assays were repeated using decreased amounts of glycosphingolipids (1 μg or less) to discern the binding preferences of LT-IIc. The appearance of a band on the autoradiogram at a concentration lower or equal to 1 μg was, thereafter, considered to be positive binding. The results obtained using these conditions are exemplified in Figures 2–3 and summarized in Table I and Supplementary Table SI. LT-IIc bound to all gangliosides that had a terminal Neu5Acα3Gal or Neu5Gcα3Gal sequence (Table I), except for ganglioside GM4 (No. 3 in Supplementary Table SI), Neu5Acα3-lactotetraosylceramide (No. 11) and the Neu5Ac-globopenta/SSEA-4 ganglioside (No. 18).

A terminal α6-linked Neu5Ac (Nos. 12 and 15 in Supplementary Table SI; Figure 2B, lane 2 and Figure 2C, lane 2) did not support binding of the LT-IIc B-subunits, and gangliosides with a disialo sequence (Neu5Acα8Neu5Acα3 or Neu5Gcα8Neu5Gcα3), such as the gangliosides GD3 (Nos. 4 and 5; Figure 3A), GD1b (Nos. 9 and 10; Figure 2A, lane 3), Neu5Acα8Neu5Acα3-/Neu5Gcα8Neu5Gcα3-neolactotetraosylceramide (Nos. 13 and 14; Figure 2C, lane 4) and Neu5Gcα8Neu5Gcα3-neolactohexaosylceramide (No. 16), were not recognized by LT-IIc.

Binding of LT-IIc B-subunits to derivatives of Neu5Gc-GM3 where the carboxyl group of the sialic acid had been converted to methylamide, ethylamide or propylamide (Lanne et al. 1995) was also evaluated (Supplemental Figure S1). All three modifications abrogated LT-IIc binding, demonstrating that the carboxyl group has a critical role in the binding process.

Comparisons of the relative binding affinity of the LT-IIc B-subunits for the various binding-active gangliosides were initially performed using dilutions of glycosphingolipids on thin-layer chromatograms. As shown in Figure 3A, no binding to the Neu5Ac-GD3 ganglioside occurred even at 2 μg, whereas the detection limits for the Neu5Ac-GM3 (Figure 3A) and Neu5Gc-GM3 gangliosides (Figure 3B) were ∼40 ng. The detection limit for the Neu5Ac-GM1 ganglioside was also 40 ng (Figure 3B), whereas the detection limits for the other binding-active gangliosides tested (Neu5Acα3-/Neu5Gcα3-neolactotetraosylceramide, Neu5Gcα3-neolactohexaosylceramide, Neu5Ac-GD1a and Neu5Ac-GT1b; Figure 3B and C) were 20 ng or below.

Binding studies using serial dilutions of selected gangliosides in microtiter wells confirmed the results from the chromatogram binding assays. The LT-IIc B-subunits bound to the ganglioside GD1a with a half-maximal binding at 80–100 ng/well (Figures 4A and 5A). This binding affinity was, therefore, on the same level as that of cholera toxin B-subunits (CTBs) binding to the GM1 ganglioside (half-maximal binding at 20 ng/well) (Figure 4B). Binding

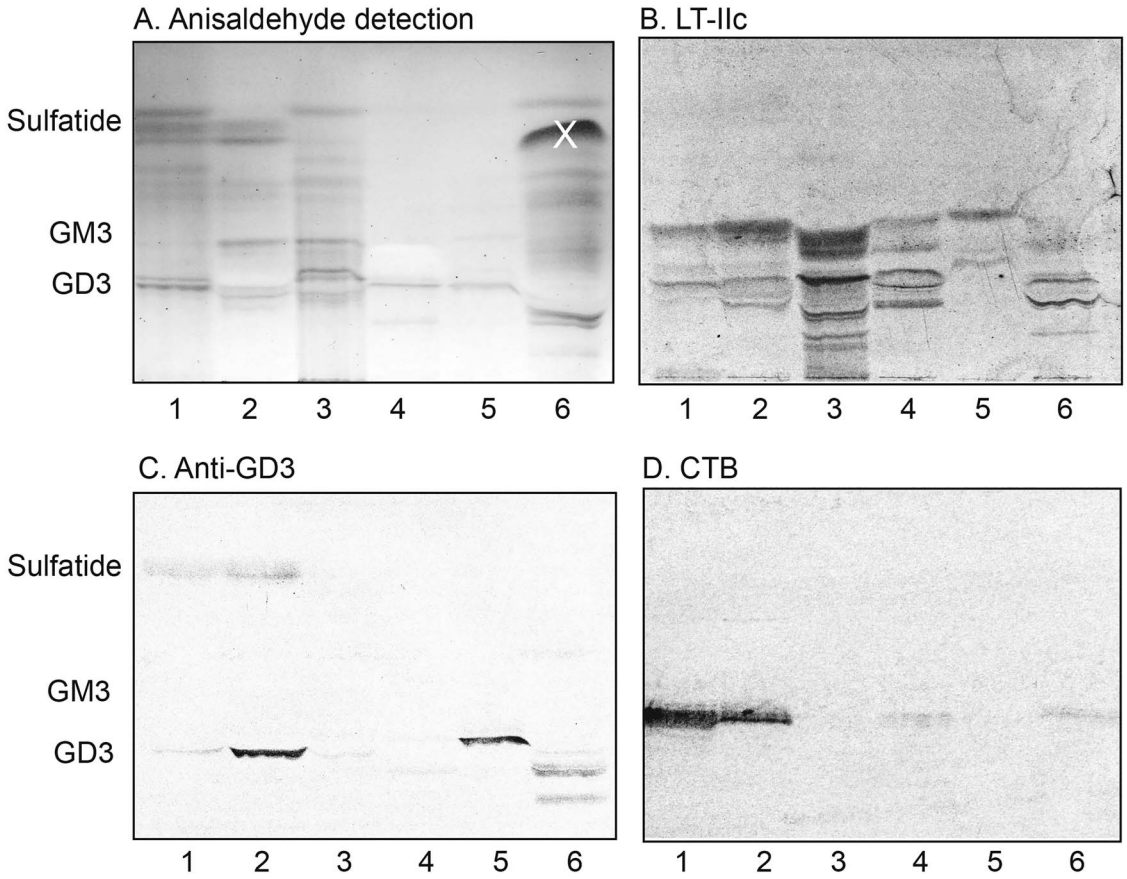

Fig. 1. Screening for LT-IIc B-subunit carbohydrate recognition by binding to mixtures of glycosphingolipids on thin-layer chromatograms. Thin-layer chromatogram stained with anisaldehyde (**A**), and autoradiograms obtained by binding of LT-IIc B-subunits (**B**), monoclonal anti-GD3 antibodies (**C**) and CTB (**D**). The chromatograms were eluted with chloroform/methanol/water 60:35:8 (by volume). The lanes were: Lane 1, acid glycosphingolipids of human small intestine 1, 20 μg; lane 2, acid glycosphingolipids of human small intestine 2, 20 μg; lane 3, acid glycosphingolipids of human neutrophils, 20 μg; lane 4, acid glycosphingolipids of rabbit thymus, 20 μg; lane 5, acid glycosphingolipids of bovine buttermilk, 20 μg; lane 6, acid glycosphingolipids of goat erythrocytes, 20 μg. The band marked with X in (**A**) is a nonglycosphingolipid contaminant. The migration levels of sulfatide, and the GM3 and GD3 gangliosides, are given to the left of the chromatograms in (**A**) and (**C**).

Table I. LT-IIc binding gangliosides[a]

Abbreviation	Structure	Detection limit
1. Neu5Ac-GM3	Neu5Acα3Galβ4Glcβ1Cer	0.04 μg
2. Neu5Gc-GM3	Neu5Gcα3Galβ4Glcβ1Cer	0.04 μg
Ganglio series		
3. Neu5Ac-GM1	Galβ3GalNAcβ4(Neu5Acα3)Galβ4Glcβ1Cer	0.04 μg
4. Neu5Ac-GD1a	Neu5Acα3Galβ3GalNAcβ4(Neu5Acα3)Galβ4Glcβ1Cer	<0.02 μg
5. Neu5Ac-GT1b	Neu5Acα3Galβ3GalNAcβ4(Neu5Acα8Neu5Acα3)Galβ4Glcβ1Cer	0.02 μg
Neolacto series		
6. Neu5Acα3-nLc4	Neu5Acα3Galβ4GlcNAcβ3Galβ4Glcβ1Cer	<0.02 μg
7. Neu5Gcα3-nLc4	Neu5Gcα3Galβ4GlcNAcβ3Galβ4Glcβ1Cer	<0.02 μg
8. Neu5Acα3-Le^x	Neu5Acα3Galβ4(Fucα3)GlcNAcβ3Galβ4Glcβ1Cer	ND
9. Neu5Ac-nLc6	Neu5Acα3Galβ4GlcNAcβ3Galβ4GlcNAcβ3Galβ4Glcβ1Cer	<0.02 μg
10. Neu5Gc-nLc6	Neu5Gcα3Galβ4GlcNAcβ3Galβ4GlcNAcβ3Galβ4Glcβ1Cer	<0.02 μg
11. Neu5Ac-VIM-2	Neu5Acα3Galβ4GlcNAcβ3Galβ4(Fucα3)GlcNAcβ3Galβ4Glcβ1Cer	ND
12. Neu5Ac-G-10	Neu5Acα3Galβ4GlcNAcβ6(Neu5Acα3Galβ4GlcNAcβ3)Galβ4Glcβ1Cer	ND

[a]Binding is defined as an intense and highly reproducible staining on the autoradiogram when 1 μg of the glycosphingolipid was applied on the thin-layer chromatogram. ND, detection limit not determined.

of LT-IIc B-subunits to Neu5Gcα3-neolactohexaosylceramide was also obtained with half-maximal binding at 200 ng/well (Figure 5A). Binding assays with Neu5Ac-GM3 and Neu5Gc-GM3 (Figure 5B) showed that the relative affinities for Neu5Ac- and Neu5Gc-terminated gangliosides were similar (100 and 300 ng/well, respectively), whereas there was no binding to the Neu5Ac-GD1b or Neu5Ac-GD3 gangliosides.

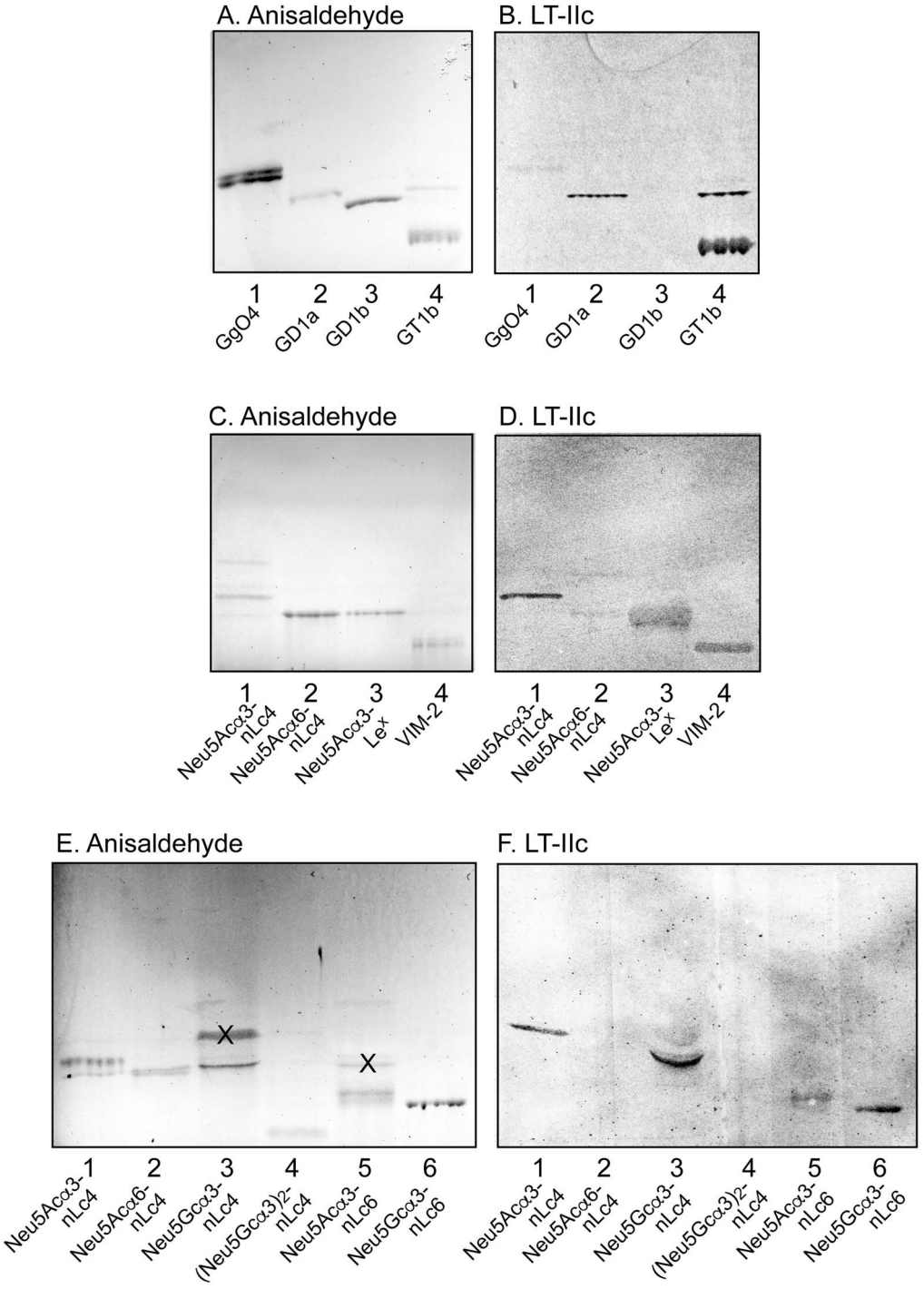

Fig. 2. Binding of LT-IIc B-subunits to reference glycosphingolipids on thin-layer chromatograms. Thin-layer chromatograms stained with anisaldehyde (**A, C** and **E**), and autoradiograms obtained by binding of LT-IIc B-subunits (**B, D** and **F**). The chromatograms were eluted with chloroform/methanol/water 60:35:8 (by volume). The lanes on a and B were: Lane 1, Gangliotetraosylceramide (GgO4; Galβ3GalNAcβ4Galβ4Glcβ1Cer), 2 μg; lane 2, GD1a ganglioside (Neu5Acα3Galβ3GalNAcβ4(Neu5Acα3)Galβ4Glcβ1Cer), 1 μg; lane 3, GD1b ganglioside (Galβ3GalNAcβ4(Neu5Acα8Neu5Acα3)Galβ4Glcβ1Cer), 1 μg; lane 4, GT1b ganglioside (Neu5Acα3Galβ3GalNAcβ4(Neu5Acα8Neu5Acα3)Galβ4Glcβ1Cer), 1 μg. The lanes on **C** and **D** were: Lane 1, Neu5Acα3-neolactotetraosylceramide (Neu5Acα3-nLc4; Neu5Acα3Galβ4GlcNAcβ3Galβ4Glcβ1Cer), 1 μg; lane 2, Neu5Acα6-neolactotetraosylceramide (Neu5Acα6-nLc4; Neu5Acα6Galβ4GlcNAcβ3Galβ4Glcβ1Cer), 1 μg; lane 3, Neu5Acα3-Le^x ganglioside (Neu5Acα3-Le^x; Neu5Acα3Galβ4(Fucα3)GlcNAcβ3Galβ4Glcβ1Cer), 1 μg; lane 4, VIM-2 ganglioside (Neu5Acα3Galβ4GlcNAcβ3Galβ4(Fucα3)GlcNAcβ3Galβ4Glcβ1Cer), 1 μg. The lanes on **E** and **F** were: Lane 1, Neu5Acα3-neolactotetraosylceramide (Neu5Acα3-nLc4; Neu5Acα3Galβ4GlcNAcβ3Galβ4Glcβ1Cer), 1 μg; lane 2, Neu5Acα6-neolactotetraosylceramide (Neu5Acα6-nLc4; Neu5Acα6Galβ4GlcNAcβ3Galβ4Glcβ1Cer), 1 μg; lane 3, Neu5Gcα3-neolactotetraosylceramide (Neu5Gcα3-nLc4; Neu5Gcα3Galβ4GlcNAcβ3Galβ4Glcβ1Cer), 1 μg; lane 4, Neu5Gcα8Neu5Gcα3-neolactotetraosylceramide ((Neu5Gcα3)$_2$-nLc4; Neu5Gcα8Neu5Gcα3Galβ4GlcNAcβ3Galβ4Glcβ1Cer), 1 μg; lane 5, Neu5Acα3-neolactohexaosylceramide (Neu5Acα3-nLc6; Neu5Acα3Galβ4GlcNAcβ3Galβ4GlcNAcβ3Galβ4Glcβ1Cer), 1 μg; lane 6, Neu5Gcα3-neolactohexaosylceramide (Neu5Gcα3-nLc6; Neu5Gcα3Galβ4GlcNAcβ3Galβ4GlcNAcβ3Galβ4Glcβ1Cer), 1 μg. The bands marked with X in (**E**) are nonglycosphingolipid contaminants.

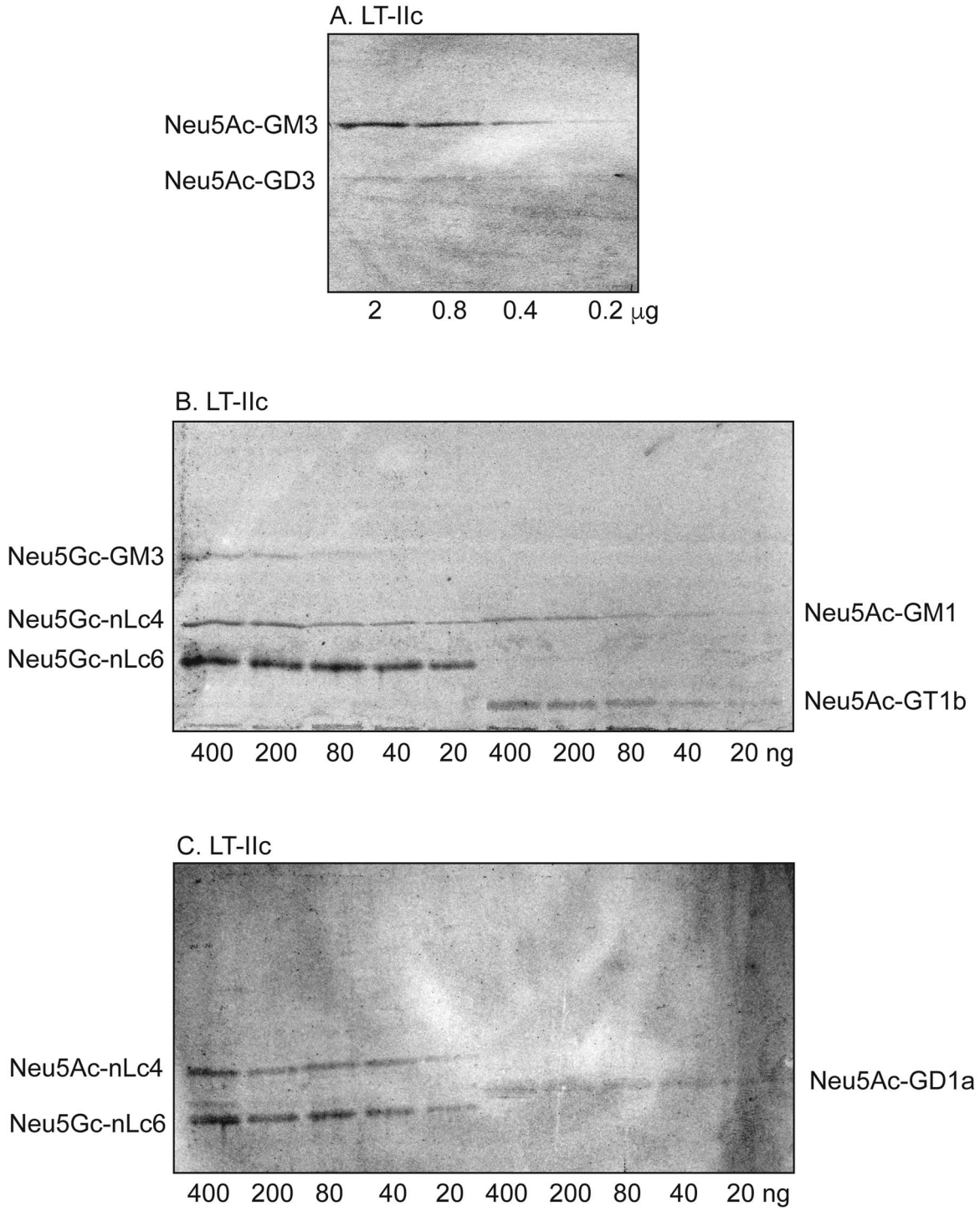

Fig. 3. Binding of LT-IIc B-subunits to dilutions of gangliosides on thin-layer chromatograms. Autoradiograms obtained by binding of LT-IIc B-subunits (**A-C**). The chromatograms were eluted with chloroform/methanol/water 60:35:8 (by volume). Neu5Acα3-GM3, Neu5Acα3Galβ4Glcβ1Cer; Neu5Acα3-GD3, Neu5Acα8Neu5Acα3Galβ4Glcβ1Cer; Neu5Gcα3-GM3, Neu5Gcα3Galβ4Glcβ1Cer; Neu5Gcα3-nLc4, Neu5Gcα3Galβ4GlcNAcβ3Galβ4Glcβ1Cer; Neu5Gcα3-nLc6, Neu5Gcα3Galβ4GlcNAcβ3Galβ4GlcNAcβ3Galβ4Glcβ1Cer; Neu5Ac-GM1, Galβ3GalNAcβ4(Neu5Acα3)Galβ4Glcβ1Cer; Neu5Ac-GT1b, Neu5Acα3Galβ3GalNAcβ4(Neu5Acα8Neu5Acα3)Galβ4Glcβ1Cer; Neu5Acα3-nLc4, Neu5Acα3Galβ4GlcNAcβ3Galβ4Glcβ1Cer; Neu5Ac-GD1a, Neu5Acα3Galβ3GalNAcβ4(Neu5Acα3)Galβ4Glcβ1Cer.

Glycoprotein binding by LT-IIc B-subunits

The minimal Neu5Acα3Gal or Neu5Gcα3Gal sequence required for LT-IIc B-subunit glycosphingolipid binding is also present on many glycoproteins (Lowe and Marth 1999). Therefore, the potential binding of LT-IIc to glycoproteins was examined. Fetuin, the major glycoprotein in fetal calf serum, and the desialylated form of fetuin, was employed as model proteins. Here, a distinct binding of LT-IIc B-subunits to fetuin was obtained, whereas no binding to asialofetuin was detected (Supplemental Figure S2).

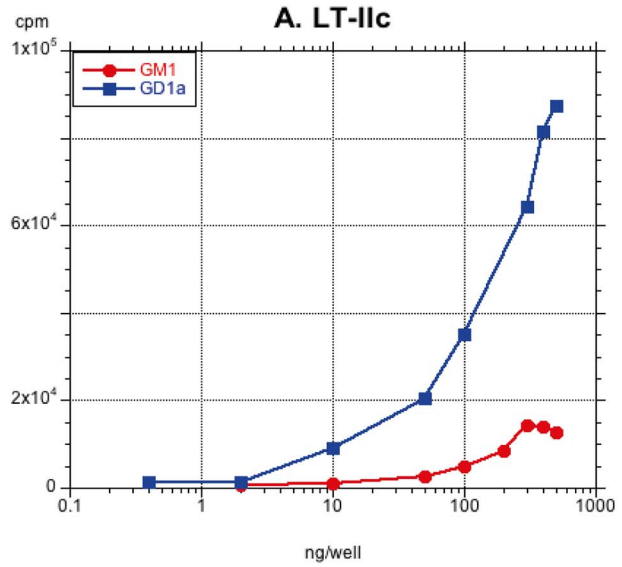

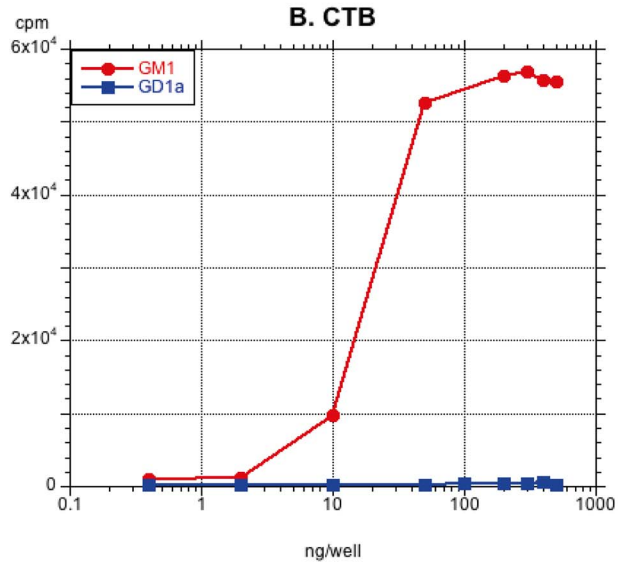

Fig. 4. Binding of ^{125}I-labeled B-subunits of LT-IIc and CT to serial dilutions of glycosphingolipids in microtiter wells. Data are expressed as mean values of triplicate determinations.

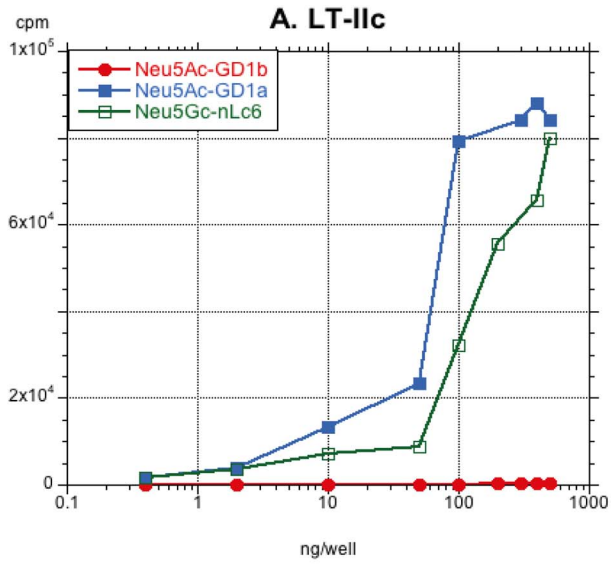

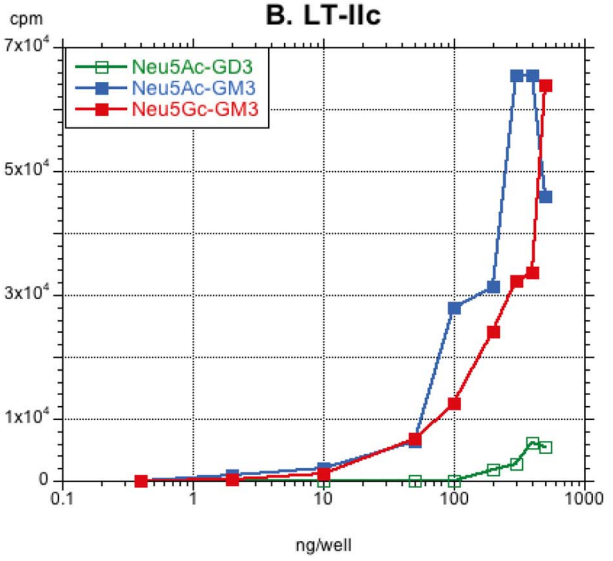

Fig. 5. Binding of ^{125}I-labeled LT-IIc B-subunits to serial dilutions of glycosphingolipids in microtiter wells. Data are expressed as mean values of triplicate determinations.

Inhibition of LT-IIc ganglioside binding

To evaluate the potential effect of sialylated saccharides on ganglioside binding, ^{125}I-labeled LT-IIc B-subunits were incubated with 50 mM Neu5Acα3-lactose (Neu5Acα3Galβ4Glc), or with PBS only, before binding to Neu5Ac-GM3, Neu5Acα3-neolactotetraosylceramide, Neu5Gcα3-nelactohexaosylceramide and Neu5Ac-GD1a in the microtiter well assay. Preincubation with the Neu5Acα3-lactose saccharide severely decreased the binding of LT-IIc subunits to the four gangliosides (Figure 6).

Binding of LT-IIc to gangliosides of human small intestine and human leukocytes

LT-IIc is both a diarrheagenic agent and a potent adjuvant (Nawar et al. 2011), and thus interacts with both intestinal cells and lymphocytes. In an attempt to identify LT-IIc binding gangliosides from human target cells, we investigated the binding of LT-IIc B-subunits to acid glycosphingolipids obtained from human small intestine and human leukocytes. Acid glycosphingolipids from human lymphocytes were not available.

In the acid glycosphingolipid fraction from human small intestine (Figure 7, lane 1), a distinct binding of LT-IIc B-subunits to three compounds, co-migrating with the GM3 ganglioside, GD1a and sialyl-neolactohexaosylceramide, was observed. A distinct binding to several gangliosides of human leukocytes was also found (Figure 7, lane 2). In this case, the recognized compounds migrated at the level of the GM3 ganglioside, sialyl-neolactotetraosylceramide, sialyl-neolactohexaosylceramide and below.

LT-IIc B-subunit apo crystal structure

Several crystallization conditions were identified for the B-pentamer in the absence of the A polypeptide after

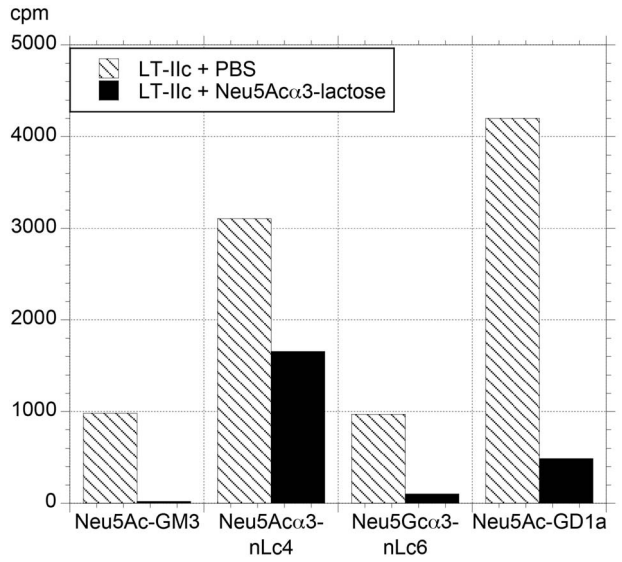

Fig. 6. Inhibition of LT-IIc B-subunit ganglioside binding by Neu5Acα3-lactose. Binding of ^{125}I-labeled LT-IIc B-subunits incubated with 50 mM Neu5Acα3-lactose (Neu5Acα3Galβ4Glc), or with PBS, to Neu5Ac-GM3, Neu5Acα3-neolactotetraosylceramide, Neu5Gcα3-nelactohexaosylceramide and Neu5Ac-GD1a (10 ng/well) in the microtiter well assay. Data are expressed as mean values of triplicate determinations.

incubation with different oligosaccharides (GD1a saccharide, LSTd/sialyl-lacto-*N*-neotetraose d pentasaccharide, and sialyl-lactose) using the HTXlab platform, EMBL Grenoble, France, which were reproduced and optimized manually. Many conditions did not produce crystals with suitable diffraction for evaluation (> 3.5 Å). Needle clusters were obtained using sodium formate as precipitant and citric acid pH 4.0–5.0 as buffer for the B-pentamer preincubated with GD1a. Data were collected on single broken needle and statistics can be found in Supplementary Table SII. The structure was resolved at 2.3 Å by molecular replacement using LT-IIb B-subunit as model (PDB ID 5G3L) (Zalem et al. 2016). Only one classical B-subunit pentamer of the bacterial enterotoxin was observed in the asymmetric unit with the five protomers displaying the same conformation with a root mean square deviation (rsmd) between 0.14 and 0.2 Å (Figure 8A). In the five protomers, all 104 amino acids could be traced including the C-terminal 6 His-tag, but no sugar could be observed in the electron density map.

Each protomer is composed of two three-stranded antiparallel β-sheets with one small α-helix at the N-terminus located on the outside of the pentameric ring and one long α-helix forming the interior of the B-subunit pore. The crystal packing revealed that the pentamers were stacked on top of each other, resulting in the His-tag hindering the oligosaccharide binding in the pentamer below (Figure 8B), which explains why no density for sugar could be observed.

LT-IIc B-subunit – LSTd/sialyl-lacto-*N*-neotetraose d complex

During crystallization screening and testing different crystal forms, rod-like crystals were observed when lithium sulfate was used as precipitant and only for LT-IIc pentamers preincubated with LSTd/sialyl-lacto-*N*-neotetraose d. Data were collected at 2 Å resolution in $P2_12_12_1$ space group. The asymmetric unit contains two pentamers and all amino acids were modeled for each protomer apart from the last five histidines of the six His C-terminal tag, where no electron density could be observed. Inspection of the electron density revealed ligand binding in the sialic acid binding site observed previously for LT-IIb B-subunits (Zalem et al. 2016). The sialic acid moiety was modeled in all binding sites for one pentamer with additional three sugar units of LSTd/sialyl-lacto-*N*-neotetraose d in one binding site (Figure 9A). In the other pentamer, LSTd/sialyl-lacto-*N*-neotetraose d tri-, tetra- and pentasaccharides could be build, whereas in the remaining sites, the electron density was of insufficient quality to model any ligand, probably as a result of low occupancy and disorder (Figure 9B). It should be noted that the sugar moieties could be modeled essentially when they were stabilized by crystal contacts through stacking interactions with the sugar units from a symmetric LSTd/sialyl-lacto-*N*-neotetraose d. Otherwise, the other carbohydrate moieties were exposed to the solvent and too disordered with no electron density visible to enable modeling (Figure 9B).

The contacts with the sialic acid moieties of the gangliosides were quite limited and consisted of direct hydrogen bonds located between its carboxylate moiety with Thr14 main chain nitrogen and side chain oxygen, and between the O4 hydroxyl and the main chain nitrogen of Lys32 and the side chain oxygen from Asn31 (Figure 9C). The *N*-acetyl moiety of the sialic acid makes hydrophobic contact with the ring of Trp92.

The LT-IIc B-subunit has 53% sequence identity with the LT-IIb B-subunit, and their structures are very similar with a rsmd of 0.8 Å for the 491 aligned residues of the pentamer (Figure 10A). Their primary carbohydrate binding sites are located in a shallow grove at the top of the pentamer at the interface between protomers. Their interactions with sialic acid are conserved and also the amino acids involved in side chain interactions (Thr14, Trp92 and Asn31). Most of the amino acids forming these primary binding sites are conserved, but we noted two main differences. At position 32, LT-IIc presents a lysine but its side chain is very disordered and could not be built into density. It could interact with the sialic acid moiety but this is hindered in the present structure by potential steric clashes with notably LSTd from a symmetric molecule. The peptidic chain has also a different orientation than in LT-IIb (Figure 10B). The loop between strand β5 and β6 presents notably a tyrosine at position 86 which makes the binding site more enclosed (Figure 10B). The hydroxyl interacts with the glycerol moiety of the sialic acid depending of its orientation, but this interaction was not conserved in all occupied binding sites. This also reduces the flexibility of the glycerol moiety contrary to LT-IIb where a serine is present.

Contrary to LT-IIb, LT-IIc does not present a secondary binding site for sialic acid. The overlay of the two complexed structures revealed that it could be due to the nonconservation of the sequence in the bridging strand β4 and helix α2, which would lead to a different binding surface (Figure 10A and C). There is no major variation in the main chain conformation but changes in the side chain directly impact the network of interactions and the overall architecture. Arg51, which was making an important hydrogen bond and hydrophobic interactions with the sialic acid carboxylate moiety, is replaced in LT-IIc by a glycine with no possible interactions. Tyr52 is conserved as well as its orientation and possible interactions. Change of Ser50 into proline or Asp54 into a tyrosine in LT-IIc will restrict the flexibility of the glycerol moiety and hinder

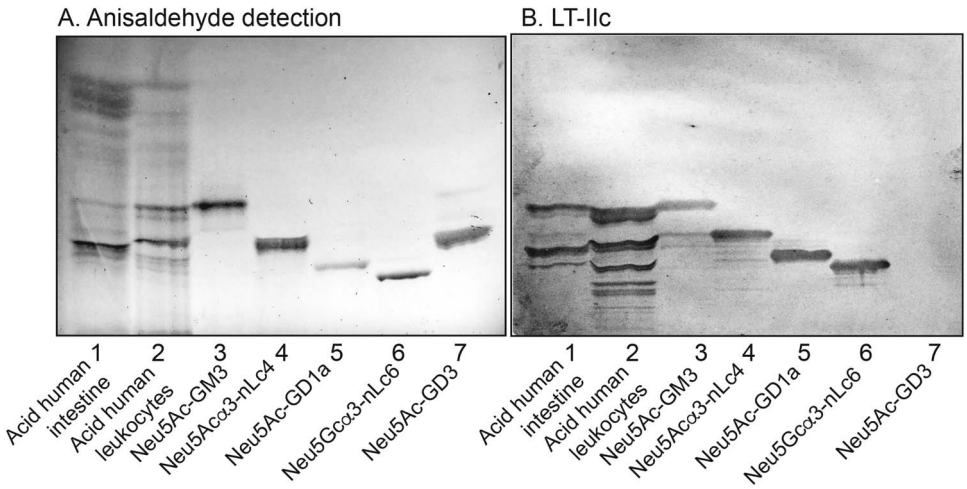

Fig. 7. Binding of LT-IIc B-subunits to gangliosides of human small intestine and human leukocytes. Thin-layer chromatogram stained with anisaldehyde by (**A**), and autoradiogram obtained by binding of LT-IIc B-subunits (**B**). The chromatograms were eluted with chloroform/methanol/water 60:35:8 (by volume). The lanes were: Lane 1, acid glycosphingolipids of human small intestine; lane 2, acid glycosphingolipids of human leukocytes; lane 3, reference Neu5Ac-GM3 (Neu5Acα3Galβ4Glcβ1Cer); lane 4, reference Neu5Acα3-neolactotetraosylceramide (Neu5Acα3-nLc4; Neu5Acα3Galβ4GlcNAcβ3Galβ4Glcβ1Cer); lane 5, reference Neu5Ac-GD1a (Neu5Acα3Galβ3GalNAcβ4(Neu5Acα3)Galβ4Glcβ1Cer); lane 6, reference Neu5Gcα3-neolactohexaosylceramide (Neu5Gcα3-nLc6; Neu5Gcα3Galβ4GlcNAcβ3Galβ4GlcNAcβ3Galβ4Glcβ1Cer); lane 7, reference Neu5Ac-GD3 (Neu5Acα8Neu5Acα3Galβ4Glcβ1Cer). On the chromatogram in (**A**) 40 μg was applied in lanes 1 and 2, and 4 μg in lanes 3–7, whereas the chromatogram in (**B**) had 40 μg in lanes 1 and 2, and 0.4 μg in lanes 3–7.

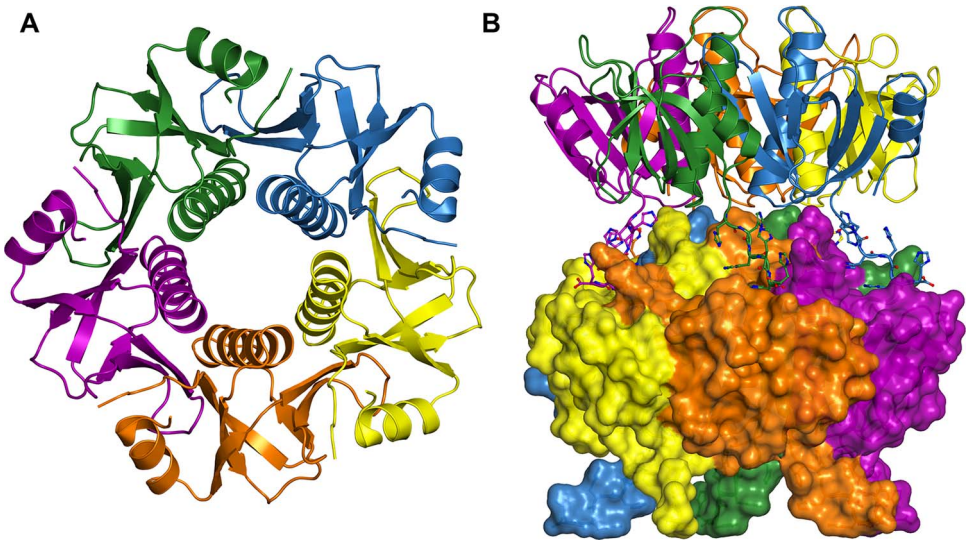

Fig. 8. Cartoon representation of LT-IIc pentamer colored by protomer. (**A**) Side view of the pentamer with representation of the his tag in balls and sticks and surface representation of the symmetric pentamer showing how the his tag blocks the primary sialic acid binding site (**B**).

water mediated H-bond with the O4 hydroxyl, respectively (Figure 10C).

Discussion

In this study, we investigated the carbohydrate binding specificity of LT-IIc by means of solid phase glycosphingolipid binding studies. By binding to a variety of glycosphingolipids separated on thin-layer chromatograms, we found that LT-IIc binds with high affinity to gangliosides with a terminal Neu5Acα3Gal or Neu5Gcα3Gal sequence, as e.g. the gangliosides GM3, GD1a and Neu5Acα3-/Neu5Gcα3-neolactotetraosylceramide and Neu5Acα3-/Neu5Gcα3-neolactohexaosylceramide. The Neu5Ac variant of these gangliosides are all present in human small intestine (Zalem et al. 2016), and thus may function as attachment factors for the B-subunits. Furthermore, the binding of LT-IIc B-subunits to fetuin, but not to asialofetuin, suggests that sialylated intestinal glycoproteins may also be involved in target cell binding of the toxin.

Most gangliosides with a terminal Neu5Acα3Gal or Neu5Gcα3Gal sequence were recognized by LT-IIc B-subunits, indicating that Neu5Ac/Neu5Gcα3Gal is the minimum binding epitope. There were, however, some gangliosides carrying this sequence that were nonbinding (the GM4 ganglioside, Neu5Acα3-lactotetraosylceramide, and the Neu5Ac-globopenta/SSEA-4 ganglioside). The GM4 ganglioside has a relatively short carbohydrate chain and might not be accessible for the B-subunits. The nonbinding of Neu5Ac α3-lactotetraosylceramide, and the Neu5Ac-globopenta/SSEA-4 ganglioside, could be due to conformational limitations. Molecular modeling has shown that the presentation of

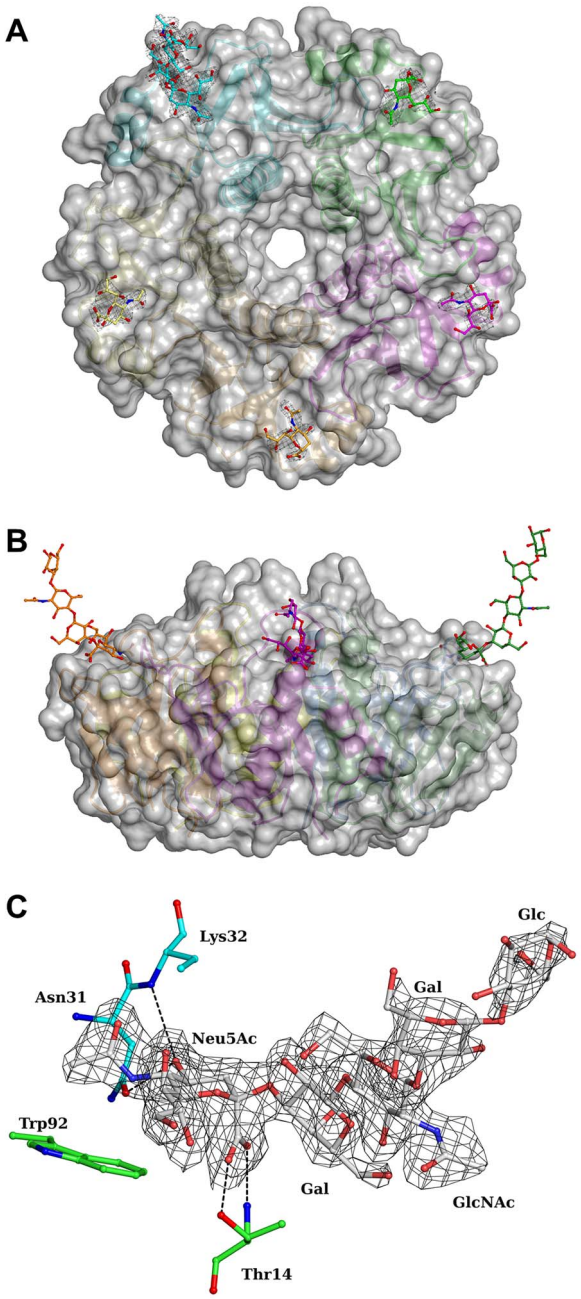

Fig. 9. Sialic acid recognition by the B-subunits of LT-IIc. Surface representation of the second pentamer with 2Fo-fc electron density map displayed at 1σ (0.25eÅ^3) around the bound sugar moieties (**A**). Side view of the surface representation for the first pentamer of LT-IIc B subunit with LSTd/sialyl-lacto-*N*-neotetraose d displayed in balls and sticks (**B**). Zoom in the interactions in the primary sialic acid binding site with electron density displayed around the oligosaccharide at 1σ (**C**). H bonds are represented by dashed lines.

terminal carbohydrates on type 1 and type 2 core chains differs (Coddens et al. 2009), thereby suggesting that the Neu5Acα3Gal epitope might not be fully accessible on type 1 core chains. The Galα4Gal sequence found in the Neu5Ac-globopenta/SSEA-4 ganglioside bends the carbohydrate chain, making the terminal carbohydrate units toward the ceramide part of the molecule (Strömberg et al. 1991), which may explain why this ganglioside is not recognized by the LT-IIc B-subunits.

LT-IIc is a potent adjuvant that potentiate mucosal and systemic T cell responses against unrelated co-administered antigens (Nawar et al. 2011; Hu et al. 2014). Thus, lymphocytes are also target cells of LT-IIc. The major ganglioside of human peripheral blood lymphocytes and monocytes is Neu5Ac-GM3. These immune cells also express gangliosides having neolacto core chains (Macher et al. 1981; Kiguchi et al. 1990), whereas gangliosides based on ganglio core chains, e.g. GM1 and GD1a, are absent (Yohe et al. 2001). Thus, the binding of LT-IIc to Neu5Acα3-neolacto gangliosides, along with Neu5Ac-GM3 binding, may also have a critical role in the immunomodulatory activities of the protein.

At the structural level, LT-IIc is almost identical to LT-IIb, all secondary structure elements are conserved. The conformation of the loops is similar despite that they are very dissimilar in sequence. The recognition of the Neu5Acα3Gal epitope is also very similar. No secondary binding site could be observed for LT-IIc and is not expected after comparison with LT-IIb.

LT type 1 B-subunits bind to glycoconjugates with terminal *N*-acetyllactosamine (Orlandi et al. 1994; Teneberg et al. 1994), in addition to binding GM1 ganglioside. Furthermore, recent studies demonstrated that the B pentamer of CT (CTB) binds to fucosylated proteins (Wands et al. 2015; Cervin et al. 2015; Wands et al. 2018). In this investigation, binding to pure nonacid reference glycosphingolipids was also examined, but no binding of LT-IIc to these glycosphingolipids was observed (data not shown). It should be noted, however, that binding of CTB to fucosylated glycans was obtained only when these moieties were expressed on glycoproteins, i.e. no binding of CTB to fucosylated glycosphingolipids was observed (Cervin et al. 2015). LT-IIc recognized two fucosylated gangliosides (sialyl-Lewis^x hexaosylceramide and the VIM-2 ganglioside), but this binding was most likely due to their terminal Neu5Acα3Gal sequence.

Analysis of a large collection of *E. coli* strains producing type II enterotoxins showed that LT-IIc toxin genes were found in the majority of the isolates, whereas LT-IIa and LT-IIb toxin types were found in only 6%and 2% of isolates, respectively (Jobling and Holmes 2012). Our definition of the structural basis for receptor ganglioside recognition by LT-IIc may contribute toward the development of new antibiotic-independent treatment strategies and design of detoxified enterotoxin-based adjuvants.

Materials and methods

Production of LT-IIc B-subunits for glycosphingolipid binding studies

A synthetic LT-IIc B-subunit gene (ATG-Biosynthetics, Merzhausen, Germany) was cloned into the pMB1-based expression vector pML-λcI857 constructed in our laboratory. Transcription of the B-subunit gene in the resulting plasmid, pML-LTBIIc/λ/cI857, is controlled by the temperature-sensitive cI_{857} repressor and initiated from the λP_L promoter. The cI_{857} repressor is active at 30°C, but is inactivated at 42°C, allowing temperature-regulated expression of the protein. In the final construct, the region encoding the signal peptide of the protein was removed. Thus, the mature protein is retained in the cytoplasm where it accumulates as inclusion bodies when expression is induced.

E. coli strain BL21 carrying pML-LTBIIc/λ/cI857 was cultured overnight in 25 mL of LB broth supplemented with

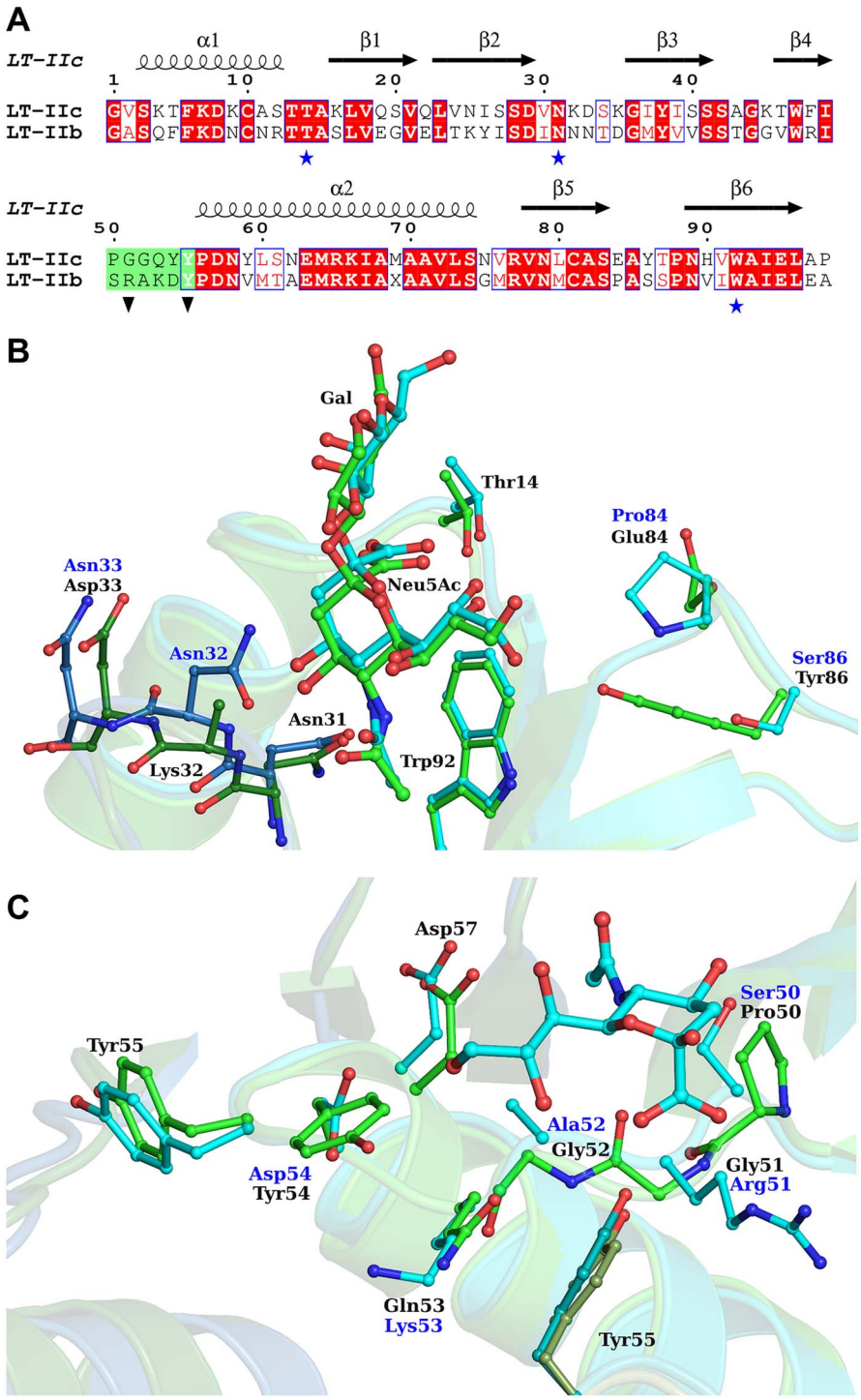

Fig. 10. Comparison of the B-subunits of LT-IIc and LT-IIb. Sequence alignment for the B-subunits of LT-IIc and LT-IIb (**A**). Figure drawn with Espript 3.0 (Robert and Gouet 2014). Zoom in the overlay of the primary (**B**) and secondary sialic acid binding site (**C**). Carbon atoms of the LT-IIc B-subunit are colored in green and those of the LT-IIb B-subunit in cyan.

100 μg/mL ampicillin at 30°C with shaking at 180 RPM. About 5 mL of the overnight starter were used to inoculate 500 mL of fresh LB/ampicillin medium and the culture was incubated at 30°C with shaking at 180 RPM until the OD_{600} value reached ~0.4. The temperature was then raised to 42°C, and the flasks were incubated for another 3–4 h to induce LT-IIc B-subunit expression as cytoplasmic inclusion bodies. Cells were pelleted at 13,000 × g and resuspended with 50 mM Tris/HCl (pH 8). Lysozyme and EDTA were added to final concentrations of 100 mg/mL and 1 mM, respectively, and the suspension was incubated at RT for 30 min. Triton X-1000 was added to a final concentration of 0.1%, and $MgCl_2$ to a final concentration of 10 mM. DNA was degraded by the addition of a small amount of DNase (Roche, Basel, Switzerland). The mixture was incubated at RT for 15 min, after which Complete Protease Inhibitor (Roche) was added

according to the manufacturer's instructions. Finally, the cells were completely disrupted by sonication performed on ice for ~5 min with 2 s pulses and 2 s intervals, at 60% amplitude (Vibra-Cell™; Sonics & Materials, Inc., Newtown, CT). The inclusion bodies were harvested by centrifugation at 5000 × g for 10 min and washed with ice cold phosphate-buffered saline (PBS; pH 7.3). The pellet was thoroughly resuspended in minimal volume of double deionized water, after which the inclusion bodies were dissolved by addition of 6.5 M urea. The solution was gently agitated overnight on a shaker at 4°C. Any undissolved debris was removed by centrifugation at 48,000 × g for 30 min.

The protein was refolded by dialysis against 50 mM sodium carbonate buffer (Na_2CO_3, pH 9) containing diminishing amounts of urea until no urea was left in the buffer. The solution was centrifuged for another 30 min at 48,000 × g, after which the supernatant underwent sterile filtration through a 0.22 μm filter. Purification of the assembled protein was performed by ion-exchange chromatography (Resource™ Q; Cytiva, Uppsala, Sweden), followed by size-exclusion chromatography (HiLoad™ 16/600 Superdex 200 pg; Cytiva), according to the protocols of the manufacturer (NGC™ Chromatography System; Bio-Rad, Hercules, CA). The protein preparation was analyzed on 14%Tris/glycine gel (Invitrogen/Thermo Fischer Scientific, Stockholm, Sweden) stained using Coomassie Brilliant Blue R-250.

Radiolabeling

Aliquots of 50 μg protein were labeled with ^{125}I by the Iodogen method according to the manufacturer's instructions (Pierce/Thermo Fischer Scientific, Stockholm, Sweden). The specific activity of the protein was 2000 cpm–4000 cpm/μg protein.

Reference glycosphingolipids

Reference glycosphingolipids were isolated and characterized by mass spectrometry and proton NMR, as described (Karlsson 1987).

Thin-layer chromatography

Aluminum- or glass-backed silica gel 60 high performance thin-layer chromatography plates (Merck, Darmstadt, Germany) were used for thin-layer chromatography. The glycosphingolipids were applied to the plates in quantities of 0.02–4 μg of pure glycosphingolipids and 20–40 μg of glycosphingolipid mixtures, and chromatographed using chloroform/methanol/water (60:35:8, by volume) as mobile phase. Chemical detection was done with anisaldehyde (Waldi 1962) or resorcinol (Svennerholm and Fredman 1980).

Chromatogram binding assays

Binding of radiolabeled LT-IIc B-subunits, and CTBs (List Labs., Campbell, CA), to glycosphingolipids on thin-layer chromatograms was done as described previously (Ångström et al. 2000). Chromatograms were dipped in diethylether/*n*-hexane (1:5 v/v) containing 0.5% (w/v) polyisobutylmethacrylate for 1 min, dried and then blocked with BSA/PBS (PBS containing 2% (w/v) bovine serum albumin and 0.1% (w/v) NaN_3) for 2 h at RT. Thereafter, the plates were incubated with ^{125}I-labeled B-subunits diluted in BSA/PBS (1–5 × 10^3 cpm/μl) for another 2 h at RT. After washing six times with PBS, and drying, the thin-layer plates were autoradiographed for 12 h using XAR-5 X-ray films (Carestream/Sigma-Aldrich, St. Louis, MO).

Binding assays with monoclonal anti-GD3 antibodies (BD Biosciences, Stockholm, Sweden) to glycosphingolipids separated on thin-layer chromatograms were performed, as described (Barone et al. 2013) using ^{125}I-labeled monoclonal anti-mouse antibodies (Z0259; DakoCytomation Norden A/S, Glostrup, Denmark) for detection.

Binding to glycosphingolipids in microtiter wells

Binding of ^{125}I-labeled LT-IIc B-subunits, and CTB, to glycosphingolipids in microtiter wells was performed as previously described (Ångström et al. 2000). In short, 50 μl of serial dilutions (each dilution in triplicate) of pure glycosphingolipids in methanol were applied to microtiter wells (Costar; Corning, NY). When the solvent had evaporated, the wells were blocked for 2 h at RT with 200 μl of BSA/PBS. Thereafter, the wells were incubated for 4 h at RT with 50 μl of ^{125}I-labeled B-subunits (2 × 10^3 cpm/μl) diluted in BSA/PBS. After washing six times with PBS, the wells were cut out and the radioactivity counted in a gamma counter.

Glycoprotein binding assays

Fetuin and asialofetuin (Sigma-Aldrich, St. Louis, MO) were diluted to 1, 2.5 and 5 mg/mL in PBS, and 12 μL of the protein samples were mixed with 12 μL of 4 × LDS sample buffer (NuPAGE/Thermo Fischer Scientific, Stockholm, Sweden), supplemented with 200 mM dithiothreitol for reducing conditions and heated at 95°C for 5 min. The proteins were separated by electrophoresis on 4–12% Bis–Tris gels (NuPAGE) with precision protein standards (Biorad, Hercules, CA) as markers and stained either with ImperialTM Protein Stain (Thermo Scientific, Stockholm, Sweden), or transferred to 0.2 μm nitrocellulose membranes (Biorad). The membranes were blocked using BSA/PBS containing 0.1% Tween 20 (BSA/PBS/Tween) for 1 h and subsequently incubated with radiolabeled LT-IIc protein dissolved in BSA/PBS/Tween (~2 × 10^6 cpm/mL) for 3 h or overnight. Membranes were washed six times with PBS, dried and autoradiographed for 6 h.

Inhibition studies

For inhibition experiments, ^{125}I-labeled LT-IIc B-subunits in BSA/PBS (4 × 10^3 cpm/μl) were incubated with Neu5Acα3-lactose (Neu5Acα3Galβ4Glc; Elicityl, Crolles, France), or with PBS only, for 2 h at RT. The solutions were diluted to 1 × 10^3 cpm/μl and used in the microtiter well assay with wells coated with 10 ng ganglioside/well.

Production of LT-IIc B-subunits for crystallization studies

The plasmid encoding LT-IIc B-subunits (pJCH3.2) was previously engineered (Nawar et al. 2011). The plasmid was introduced into *E. coli* DH5αF'Kan (Life Technologies, Inc., Gaithersburg, MD) and expression was induced by addition of 5 mM isopropyl-β-d-thiogalactoside to the culture medium. Recombinant B-pentamers were extracted from the periplasmic space and purified to homogeneity by the use of nickel affinity chromatography and Sephacryl-100 gel filtration chromatography (VWR, Piscataway, NJ) using an ÄKTA-FPLC (Cytiva, Peapack, NJ) (Nawar et al. 2005).

Crystallization and structure determination

LT-IIc B-subunit pentamers were concentrated to the desired concentration in 20 mM Hepes 7.5 and 100 mM NaCl

using centrifugal concentration device (Vivaspin4, 3000 Da cut-off; Sartorius, Goettingen, Germany). The protein was preincubated with 1.3 mM LSTd/sialyl-lacto-*N*-neotetraose d, 0.2 mM GD1a or 3.3 mM 3-sialyl lactose (Elicityl, Crolles, France) for >15 min at RT prior to crystallization. A first screening was performed using the robotized HTXlab platform (EMBL, Grenoble, France) and 200 nanoliter sitting drops at 20°C. Hits were reproduced and optimized using the vapor diffusion method with 2 μL hanging drops consisting of one protein:one reservoir mix at 19°C. Cocrystallization of the LT-IIc pentamers at 7.5 mg/mL with GD1a led to the formation of needle clusters with solution containing 2.4–2.6 M sodium formate and 100 mM citric acid, pH 4.0 or 5.0. Single needles were cut out and transferred in 4.2 M sodium formate for cryoprotection before mounting in cryoloop and flash-freezing in liquid nitrogen.

Cocrystallization of LT-IIc pentamers performed at 4.8 mg/mL with LSTd/sialyl-lacto-*N*-neotetraose d gave hexagonal crystals using 1.5 M $LiSO_4$ and 100 mM Mes pH 6.5. Crystals were transferred into 2.5 M $LiSO_4$ before crystal mounting and freezing. Diffraction data were collected at 100 K at the SOLEIL synchrotron in Saint Aubin, France on the Proxima 1 beamline using an EIGER-X 16 M detector (Dectris AG.; Baden, Switzerland).

Data were processed using XDS and XDSme (Kabsch 2010; Legrand 2017) and were converted to structure factors using the CCP4 program suite (Winn et al. 2011) with 5% of the data selected randomly from the observed reflections and reserved for R_{free} calculation.

The apo structure of LT-IIc B-subunits was solved by molecular replacement using the pentamer of LT-IIb B-subunits (PDB ID: 5G3L) as search model in PHASER 2.8.2 (McCoy et al. 2007) after mutation and conservation of gamma atoms in CHAINSAW. The structure in complex with LSTd/sialyl-lacto-*N*-neotetraose d was solved by molecular replacement using the apo structure as model, and a search for two pentamers in the asymmetric unit in PHASER 2.8.3. After initial rebuilding with ARP/WARP (Langer et al. 2008), both models were refined using restrained maximum likelihood refinement using REFMAC 5.8.0267 and local NCS restrains (Murshudov and Nicholls 2011), iterated with manual rebuilding in Coot (Emsley and Lohkamp 2010). For the LSTd/sialyl-lacto-*N*-neotetraose d complexed structure, TLS refinement was also performed toward the end, and carbohydrates were introduced upon inspection of the electron density maps and checked using Privateer (Aguirre et al. 2015). Hydrogen atoms were added in their riding positions and used for geometry and structure factor calculations. Before deposition in the Protein Data Bank, the models were validated using both the wwPDB Validation server (http://wwpdb-validation.wwpdb.org) and Molprobity (Williams et al. 2018). Coordinates and structure factors have been deposited under PDB accession codes 7PRP and 7PRS for LT-IIc B-subunits in apo form or complex with LSTd/sialyl-lacto-*N*-neotetraose d pentasaccharide, respectively. Data quality and refinement statistics are described in Supplementary Table SII. Figures 8–10 were created using PyMOL version 2.4 (www.schrodinger.com/products/pymol).

Supplementary data

Supplementary data are available at *Glycobiology* online.

Acknowledgements

The authors thank Darja Bozic for her help in the crystallization of the apo B-subunit. This work benefited from access to the High Throughput Crystallization Facility (HTX lab), EMBL Grenoble, France, an Instruct center. Thanks to SOLEIL (St Aubin, France) for the provision of synchrotron radiation facilities as well as access to and technical assistance on Proxima 1 beamline (proposal 20191314).

Conflicts of interest

None declared.

Funding

This work was supported by iNEXT projects 1928 and 2526 funded from the European Community H2020 Programme under the project iNEXT (Grant No. 653706 to A.V.) and CNRS (A.V.), the Swedish Cancer Foundation (Grant No. 20 0759 PjF 01 H to S.T.), the National Cancer Institute, Department of Health and Human Services (Grant No. 21CA208475 to T.D.C.) and by the Breast Cancer Research Program (BCRP) from the Defense Health Program of the U.S. Department of Defense (Grant No. W81XWH-18-1-0042 to T.D.C.).

Abbreviations

CT, cholera toxin; CTB, cholera toxin B-subunits; ETEC, enterotoxigenic *E. coli*; LT, heat-labile enterotoxin; LSTd, sialyl-lacto-*N*-neotetraose d.

References

Aguirre J, Iglesias-Fernandez J, Rovira C, Davies GJ, Wilson KS, Cowtan KD. 2015. Privateer: Software for the conformational validation of carbohydrate structures. *Nat Struct Mol Biol*. **22**:833–834.

van den Akker F, Sarfaty S, Twiddy EM, Connell TD, Holmes RK, Hol WG. 1996. Crystal structure of a new heat-labile enterotoxin LT-IIb. *Structure*. **4**:665–678.

Ångström J, Bäckström M, Berntsson A, Karlsson N, Holmgren J, Karlsson K-A, Teneberg S. 2000. Novel carbohydrate binding site recognizing blood group a and B determinants in a cholera toxin/heat-labile enterotoxin B-subunit hybrid. *J Biol Chem*. **275**:3231–3238.

Barone A, Benktander J, Ångström J, Aspegren A, Björquist P, Teneberg S, Breimer ME. 2013. Structural complexity of non-acid glycosphingolipids in human embryonic stem cells grown under feeder-free conditions. *J Biol Chem*. **288**:10035–10050.

Beddoe T, Paton AW, Le Nours J, Rossjohn J, Paton JC. 2010. Structure, biological functions and applications of the AB5 toxins. *Trends Biochem*. **35**:411–418.

Berenson CS, Nawar HF, Kruzel RL, Mandell LM, Connell TD. 2013. Ganglioside-binding specificities of *E. coli* enterotoxin LT-IIc: Importance of long-chain fatty acyl ceramide. *Glycobiology*. **23**: 23–31.

Cervin J, Wands AM, Casselbrant A, Wu H, Krishnamurthy S, Cvjetkovic A, Estelius J, Coddens A, Diswall M, Ångström J *et al.* 2009. Recognition of blood group ABH type 1 determinants by the FedF adhesin of F18-fimbriated *Escherichia coli*. *J Biol Chem*. **284**: 9713–9726.

Dedic B, Sethi A, Wallom KL, Riise R, Bäckström M, Wallenius V, Platt FM, Lebens M, Teneberg S, Fändriks L *et al.* 2015. GM1 ganglioside-independent intoxication by cholera toxin. *PLoS Pathog*. **14**:e1006862.

Emsley P, Lohkamp B. 2010. Features and development of coot. *Acta Crystallogr Sect D Biol Crystallogr*. **66**:486–501.

Fan E, Merritt EA, Verlinde CL, Hol WG. 2000. AB(5) toxins: Structures and inhibitor design. *Curr Opin Struct Biol*. **10**:680–686.

Fukuta S, Magnani JL, Twiddy EM, Holmes RK, Ginsburg V. 1988. Comparison of the carbohydrate-binding specificities of cholera

toxin and *Escherichia coli* heat-labile enterotoxins LTh-I, LT-IIa, and LT-IIb. *Infect Immun*. **56**:1748–1753.
Gascon J. 2006. Epidemiology, etiology and pathophysiology of traveler's diarrhea. *Digestion*. **73**:102–108.
Hajishengallis G, Connell TD. 2013. Type II heat-labile enterotoxins: Structure, function and immunomodulatory properties. *Vet Immunol Immunopathol*. **152**:68–77.
Hauttecoeur B, Sonnino S, Ghidoni R. 1985. Characterization of two molecular species GD3 ganglioside from bovine buttermilk. *Biochim Biophys Acta*. **833**:303–307.
Holmgren J. 1973. Comparison of the tissue receptors for *Vibrio cholerae* and *Escherichia coli* enterotoxins by means of gangliosides and natural cholera toxoid. *Infect Immun*. **8**:851–859.
Hu JC, Mathias-Santos C, Greene CJ, King-Lyons ND, Rodrigues JF, Hajishengallis G, Ferreira LC, Connell TD. 2014. Intradermal administration of the type II heat-labile enterotoxins LT-IIb and LT-IIc of enterotoxigenic *Escherichia coli* enhances humoral and CD8+ T cell immunity to a co-administered antigen. *PLoS One*. **9**:e113978.
Iwamori M, Nagai Y. 1981. Ganglioside composition of rabbit thymus. *Biochim Biophys Acta*. **665**:205–213.
Jobling MG, Holmes RK. 2012. Type II heat-labile enterotoxins from 50 diverse *Escherichia coli* isolates belong almost exclusively to the LT-IIc family and may be prophage encoded. *PLoS One*. **7**:29898.
Kabsch W. 2010. XDS. *Acta Crystallogr*. **66**:125–132.
Karlsson KA. 1987. Preparation of total non-acid glycolipids for overlay analysis of receptors for bacteria and viruses and for other studies. *Methods Enzymol*. **138**:212–220.
Kiguchi K, Henning-Chubb CB, Huberman E. 1990. Glycosphingolipid patterns of peripheral blood lymphocytes, monocytes, and granulocytes are cell specific. *J Biochem*. **107**:8–14.
Kotloff KL, Platts-Mills JA, Nasrin D, Roose A, Blackwelder WC, Levine MM. 2017. Global burden of diarrheal diseases among children in developing countries: Incidence, etiology, and insights from new molecular diagnostic techniques. *Vaccine*. **35**:6783–6789.
Lamberti LM, Bourgeois AL, Fischer Walker CL, Black RE, Sack D. 2014. Estimating diarrheal illness and deaths attributable to Shigellae and enterotoxigenic *Escherichia coli* among older children, adolescents, and adults in South Asia and Africa. *PLoS Negl Trop Dis*. **8**:e2705.
Langer GG, Cohen SX, Lamzin VS, Perrakis A. 2008. Automated macromolecular model building for X-ray crystallography using ARP/wARP version 7. *Nat Protoc*. **3**:1171–1179.
Lanne B, Uggla L, Stenhagen G, Karlsson KA. 1995. Enhanced binding of enterotoxigenic *Escherichia coli* K99 to amide derivatives of the receptor ganglioside NeuGc-GM3. *Biochemistry*. **34**:1845–1850.
Legrand P. 2017. XDSME: XDS made easier. *GitHub Repos*. https://doi.org/10.5281/zenodo.837885.
Lowe JB, Marth JD. 1999. Structures common to different types of glycans. In: Varki A, Cummings R, Esko J, Freeze H, Hart G, Marth J, editors. *Essentials in glycobiology*. Cold Spring Harbor (NY): Cold Spring Harbor Laboratory. p. 211–252.
Macher BA, Klock JC, Fukuda MN, Fukuda M. 1981. Isolation and structural characterization of human lymphocyte and neutrophil gangliosides. *J Biol Chem*. **256**:1968–1974.
McCoy AJ, Grosse-Kunstleve RW, Adams PD, Winn MD, Storoni LC, Read RJ. 2007. Phaser crystallographic software. *J Appl Crystallogr*. **40**:658–674.
Murshudov GN, Nicholls RA. 2011. REFMAC 5 for the refinement of macromolecular crystal structures. *Acta Crystallogr Sect D Biol Crystallogr*. **67**:355–367.
Nawar HF, Arce S, Russell MW, Connell TD. 2005. Mucosal adjuvant properties of mutant LT-IIa and LT-IIb enterotoxins that exhibit altered ganglioside-binding activities. 2005. *Infect Immun*. **73**:1330–1342.
Nawar HF, King-Lyons ND, Hu JC, Pasek RC, Connell TD. 2010. LT-IIc, a new member of the type II heat-labile enterotoxin family encoded by an *Escherichia coli* strain obtained from a nonmammalian host. *Infect Immun*. **78**:4705–4713.
Nawar HF, Greene CJ, Lee CH, Mandall LM, Hajishengallis G, Connell TD. 2011. LT-IIc, a new member of the type II heat-labile enterotoxin family, exhibits potent immunomodulatory properties that are different from those induced by LT-IIa or LT-IIb. *Vaccine*. **29**:721–727.
Orlandi PA, Crithley DR, Fishman PH. 1994. The heat-labile enterotoxin of *Escherichia coli* binds to polylactosaminoglycan-containing receptors in CaCo-2 human intestinal epithelial cells. *Biochemistry*. **33**:12886–12895.
Robert X, Gouet P. 2014. Deciphering key features in protein structures with the new ENDscript server. *Nucleic Acids Res*. **42**:320–324.
Strömberg N, Nyholm PG, Pascher I, Normark S. 1991. Saccharide orientation at the cell surface affects glycolipid receptor function. *Proc Natl Acad Sci U S A*. **88**:9340–9344.
Stroud MR, Handa K, MEK MS, Ito K, Levery SB, Hakomori S-I, Reinhold BB, Reinhold VN. 1996a. Monosialogangliosides of human myelogenous leukemia HL60 cells and normal human leukocytes. 1. Separation of E-selectin binding from nonbinding gangliosides, and absence of sialosyl-Le^x having tetraosyl to octaosyl core. *Biochemistry*. **35**:758–769.
Stroud MR, Handa K, MEK MS, Ito K, Levery SB, Hakomori S-I, Reinhold BB, Reinhold VN. 1996b. Monosialogangliosides of human myelogenous leukemia HL60 cells and normal human leukocytes. 2. Characterization of E-selectin binding fractions, and structural requirements for physiological binding to E-selectin. *Biochemistry*. **35**:770–778.
Svennerholm L, Fredman P. 1980. A procedure for the quantitative isolation of brain gangliosides. *Biochim Biophys Acta*. **617**:97–109.
Teneberg S, Hirst TR, Ångström J, Karlsson K-A. 1994. Comparison of the glycolipid-binding specificities of cholera toxin and porcine *Escherichia coli* heat-labile enterotoxin: Identification of a receptor-active non-ganglioside glycolipid for the heat-labile toxin in infant rabbit small intestine. *Glycoconj J*. **11**:533–540.
Waldi D. 1962. Sprühreagentien für die dünnschicht-chromatographie. In: Stahl E, editor. *Dünnschicht-Chromatographie*. Berlin (Germany): Springer-Verlag. p. 496–515.
Wands AM, Fujita A, McCombs JE, Cervin J, Dedic B, Rodriguez AC, Nischan N, Bond MR, Mettlen M, Trudgian DC *et al.* 2015. Fucosylation and protein glycosylation create functional receptors for cholera toxin. *elife*. **4**:e09545.
Wands AM, Cervin J, Huang H, Zhang Y, Youn G, Brautigam CA, Matson Dzebo M, Björklund P, Wallenius V, Bright DK *et al.* 2018. Fucosylated molecules competitively interfere with cholera toxin binding to host cells. *ACS Infect Dis*. **4**:758–770.
Williams C, Headd JJ, Moriarty NW, Prisant MG, Videau LL, Deia LN, Verma V, Keedy DA, Hintze BJ, Chen VB *et al.* 2018. MolProbity: More and better reference data for improved all-atom structure validation. *Protein Sci*. **27**:293–315.
Winn MD, Ballard CC, Cowtan KD, Dodson EJ, Emsley P, Evans PR, Keegan RM, Krissinel EB, Leslie AGW, McCoy A *et al.* 2011. Overview of the CCP4 suite and current developments. *Acta Crystallogr Sect D Biol Crystallogr*. **67**:235–242.
Yohe HC, Wallace PK, Berenson CS, Ye S, Reinhold BB, Reinhold VN. 2001. The major gangliosides of human peripheral blood monocytes/macrophages: Absence of ganglio series structures. *Glycobiology*. **11**:831–841.
Zalem D, Ribeiro JP, Varrot A, Lebens M, Imberty A, Teneberg S. 2016. Chemical and structural characterization of the novel sialic acid binding site of *Escherichia coli* heat-labile enterotoxin LT-IIb. *Biochem J*. **473**:3923–3936.